

AlGaAs/GaAs HBT Model Estimation Through the Generalized Pencil-of-Function Method

B. L. Ooi, T. S. Zhou, and P. S. Kooi

Abstract—An efficient technique of extracting the small-signal model parameters of the heterojunction bipolar transistor (HBT) is proposed in this paper. The relation between the extrinsic and intrinsic model parameters, which can be employed to drastically reduce the search space, is studied in depth. For the first time, the HBT transistor is characterized by describing *S*-parameters with a set of complex exponentials using the generalized pencil-of-function method. The reliable initial values of some extrinsic elements can be determined from the set of complex exponentials. This novel approach can yield a good fit between measured and simulated *S*-parameters.

Index Terms—AlGaAs/GaAs, generalized pencil-of-function method, HBT, small-signal model.

I. INTRODUCTION

MICROWAVE-CIRCUIT computer-aided design (CAD) requires device models with excellent accuracy, especially for the active devices. The equivalent-circuit modeling approach has commonly been used to characterize active devices. In the past, different methods for the determination of the heterojunction bipolar transistor (HBT) microwave small-signal models were studied in depth and numerous improvements on the HBT equivalent-circuit parameter-extraction techniques have been proposed [1]–[7]. In these models, the conventional method requires extra measurements or some approximations and is generally difficult, inaccurate, and time consuming. Other methods, such as the optimization technique, which depends on the starting values, may result in nonunique solutions of the element values.

It is noted in [8] and [9] that there is a strong correlation between the extrinsic and intrinsic model parameters of GaAs MESFETs and, by explicitly using this correlation, a smaller optimization search space is resulted. In this paper, the strong correlation between extrinsic and intrinsic elements of the HBT transistor is explored in depth. In addition, by applying the generalized pencil-of-function (GPOF) method, we can approximate the *S*-parameters of the AlGaAs/GaAs HBT. The set of complex exponentials, which provides less data manipulation and storage, approximates the measured *S*-parameters with excellent accuracy, as it is very robust in eliminating statistical noise. Good initial values of the extrinsic elements in the HBT small-signal equivalent circuit by using this set of complex exponentials can be obtained.

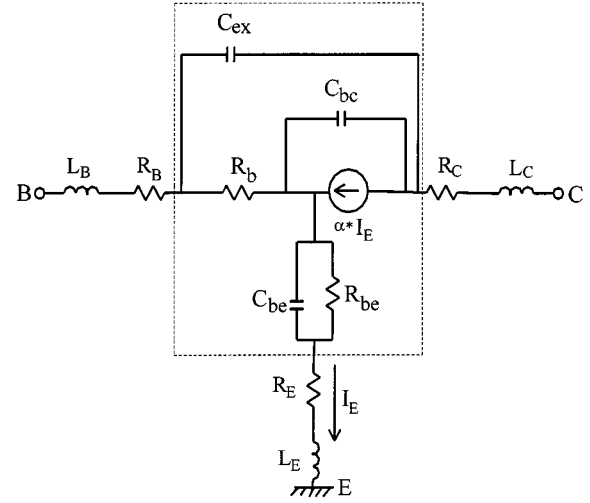


Fig. 1. Equivalent circuit of AlGaAs/GaAs HBT. Inside the dashed line denotes the intrinsic part, and the outside is the extrinsic part $\alpha = \alpha_0 \exp(-j\omega\tau)$.

II. EQUIVALENT CIRCUIT OF THE HBT TRANSISTOR

The adopted equivalent circuit is shown in Fig. 1. As indicated in this figure, the intrinsic part of the HBT transistor is the part that excludes the elements R_E , L_E , R_B , L_B , R_C , and L_C . The respective intrinsic *Z*-parameters Z_{int} are described as

$$Z_{\text{int}} = \begin{bmatrix} Z_{11} & Z_{12} \\ Z_{21} & Z_{22} \end{bmatrix} \quad (1)$$

where

$$Z_{11} = \frac{[(1-\alpha)Z_{bc} + Z_{\text{ex}}]R_b}{Z_{bc} + Z_{\text{ex}} + R_b} + Z_{be} \quad (2a)$$

$$Z_{12} = \frac{(1-\alpha)Z_{bc}R_b}{Z_{bc} + Z_{\text{ex}} + R_b} + Z_{be} \quad (2b)$$

$$Z_{21} = \frac{[-\alpha Z_{\text{ex}} + (1-\alpha)R_b]Z_{bc}}{Z_{bc} + Z_{\text{ex}} + R_b} + Z_{be} \quad (2c)$$

$$Z_{22} = \frac{(1-\alpha)Z_{bc}(Z_{\text{ex}} + R_b)}{Z_{bc} + Z_{\text{ex}} + R_b} + Z_{be} \quad (2d)$$

$$Z_{be} = \frac{R_{be}}{1 + j\omega R_{be} C_{be}} \quad (2e)$$

$$Z_{bc} = \frac{1}{j\omega C_{bc}} \quad (2f)$$

$$Z_{\text{ex}} = \frac{1}{j\omega C_{\text{ex}}} \quad (2g)$$

Manuscript received September 3, 2000.

The authors are with the Department of Electrical and Computer Engineering, National University of Singapore, Singapore 119260.

Publisher Item Identifier S 0018-9480(01)05044-X.

The extrinsic part of the transistor, which is located outside the dashed box of Fig. 1, is related to the intrinsic part through (3) and (4), shown at the bottom of this page, where Z_{total} is the overall Z -parameters and Z_{ext} is the extrinsic Z -parameters.

III. ANALYTICAL DETERMINATION OF THE EQUIVALENT-CIRCUIT ELEMENTS

As for the MESFET modeling, Ooi *et al.* [8] and Shirakawa *et al.* [9] have shown the strong dependence of the intrinsic parameters on the extrinsic parameters. In this paper, our main effort is to identify the strong correlation between the intrinsic and extrinsic elements for an HBT transistor equivalent circuit. Once this kind of correlation is obtained, the extrinsic elements can be optimized individually, and the intrinsic elements can then be synthesized from the measurement data and extrinsic elements.

The overall measured S -parameters are first converted to Z -parameters, and the intrinsic Z -parameters are obtained by using (3) and (4). Based on the adopted HBT equivalent circuit, the intrinsic elements at each frequency point are derived. The detailed expressions are given as follows:

$$\alpha_0 = \frac{\text{Re}(a)}{\cos(\omega\tau)} \quad (5a)$$

$$\tau = \frac{1}{\omega} \tan^{-1} \left[\frac{\text{Im}(a)}{\text{Re}(a)} \right] \quad (5b)$$

$$C_{\text{ex}} = \frac{\text{Re}(c)}{\omega [\text{Re}(d)\text{Im}(c) - \text{Im}(d)\text{Re}(c)]} \quad (5c)$$

$$C_{bc} = \frac{\text{Re}(d)}{\omega [\text{Im}(d)\text{Re}(c) - \text{Re}(d)\text{Im}(c)]} \quad (5d)$$

$$R_b = \frac{jb[\text{Re}(d)\text{Im}(c) - \text{Im}(d)\text{Re}(c)]}{\text{Re}(d)} \quad (5e)$$

$$R_{be} = \frac{[\text{Re}(e)]^2 + [\text{Im}(e)]^2}{\text{Re}(e)} \quad (5f)$$

$$C_{be} = \frac{-\text{Im}(e)}{\omega \{ [\text{Re}(e)]^2 + [\text{Im}(e)]^2 \}} \quad (5g)$$

$$Z_{\text{int}} = Z_{\text{total}} - Z_{\text{ext}} \quad (3)$$

$$Z_{\text{total}} = \begin{bmatrix} Z_{11}^{\text{total}} & Z_{12}^{\text{total}} \\ Z_{21}^{\text{total}} & Z_{22}^{\text{total}} \end{bmatrix}$$

$$Z_{\text{ext}} = \begin{bmatrix} R_E + R_B + j\omega L_E + j\omega L_B & R_E + j\omega L_E \\ R_E + j\omega L_E & R_E + R_C + j\omega L_E + j\omega L_C \end{bmatrix} \quad (4)$$

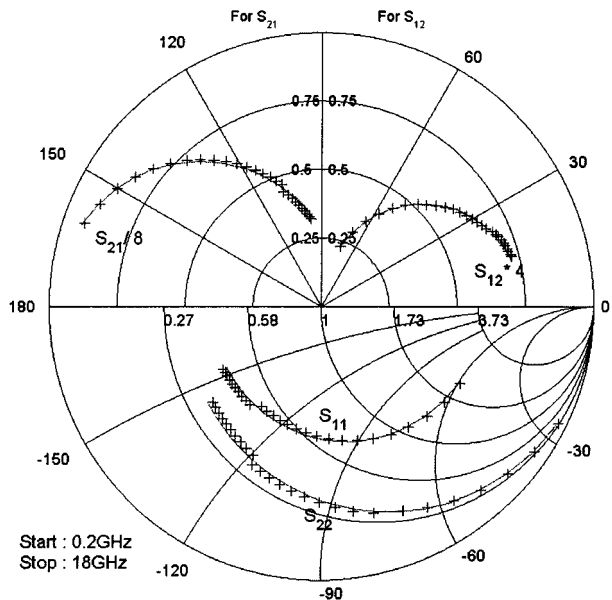


Fig. 2. Comparison of S -parameters between measured and calculated data. Solid lines indicate measured values and crosses indicate calculated values using the GPOF method.

where

$$a = \frac{Z_{12} - Z_{21}}{Z_{22} - Z_{21}} \quad (6a)$$

$$b = \frac{Z_{11} - Z_{12}}{Z_{22} - Z_{21}} \quad (6b)$$

$$c = Z_{22} - Z_{21} \quad (6c)$$

$$d = Z_{22} - Z_{21} + Z_{11} - Z_{12} \quad (6d)$$

$$e = Z_{12} + \frac{\text{Re}(Z_{22} - Z_{21} + Z_{11} - Z_{12})(Z_{12} - Z_{22})(Z_{12} - Z_{11})}{\text{Re}(Z_{22} - Z_{21})(Z_{22} - Z_{21})}. \quad (6e)$$

Equations (5a)–(6e) indicate that there is a strong correlation between the extrinsic and intrinsic elements, and the change in the intrinsic elements is solely governed by (5a)–(6e).

IV. DETERMINATION OF EXTRINSIC-ELEMENT VALUES FROM THE SET OF COMPLEX EXPONENTIALS

The GPOF method has been described in detail in [10]–[12] and, for brevity, it will not be discussed in this paper. In the GPOF method, the objective is to fit a complex function by a sum of damped complex exponentials, which is given as

$$y_k \cong \sum_{i=1}^M R_i(z_i)^k \quad (7)$$

TABLE I
CALCULATED RESIDUES AND POLES FOR $f_1(k)$, $f_2(k)$, and $f_3(k)$

Function	R_i	z_i
$f_1(k)$	1.3728×10	1.1521
	$1.1666 \times 10^{-1} \pm j1.1759 \times 10^{-1}$	$-8.1170 \times 10^{-1} \pm j2.0312 \times 10^{-1}$
	$-1.2312 \times 10^{-2} \pm j4.2263 \times 10^{-2}$	$-7.5074 \times 10^{-1} \pm j6.0473 \times 10^{-1}$
	$-2.9241 \times 10^{-1} \pm j2.9501 \times 10^{-1}$	$-5.0857 \times 10^{-1} \pm j8.5048 \times 10^{-1}$
	$-7.8010 \times 10^{-2} \pm j2.0519 \times 10^{-2}$	$6.5129 \times 10^{-1} \pm j4.2674 \times 10^{-1}$
	$8.8420 \times 10^{-1} \pm j3.3534 \times 10^{-2}$	$2.5667 \times 10^{-1} \pm j5.8600 \times 10^{-1}$
$f_2(k)$	2.3323	1.0253
	-2.2143	9.5853×10^{-1}
	$-9.9984 \times 10^{-2} \pm j4.4485 \times 10^{-2}$	$-1.0178 \pm j1.9442 \times 10^{-1}$
	$1.8587 \times 10^{-1} \pm j5.1330 \times 10^{-1}$	$5.7463 \times 10^{-1} \pm j9.8801 \times 10^{-1}$
	$3.9099 \times 10^{-2} \pm j7.5629 \times 10^{-2}$	$6.6298 \times 10^{-1} \pm j5.5764 \times 10^{-1}$
$f_3(k)$	$-8.4096 \times 10^{-2} \pm j9.1394 \times 10^{-2}$	$-4.9938 \times 10^{-1} \pm j4.7516 \times 10^{-1}$
	7.1000	1.0011
	-2.6449 $\times 10$	-6.4959×10^{-1}
	7.9217	-1.3274×10^{-1}
	$2.3445 \times 10^{-1} \pm j2.2112 \times 10^{-2}$	$8.0385 \times 10^{-1} \pm j4.2205 \times 10^{-1}$
	$5.0916 \times 10^{-1} \pm j4.7298 \times 10^{-2}$	$3.7975 \times 10^{-1} \pm j8.0370 \times 10^{-1}$
	3.4947 $\pm j3.8626$	$-1.7745 \times 10^{-1} \pm j7.4907 \times 10^{-1}$

where $k = 0, 1, \dots, N - 1$ is the number of sampling data, R_i is the residue, z_i denotes the pole, and M is the number of singular values σ_i of Y_1 [10] that satisfies the ratio $\sigma_i/\sigma_{\max} \geq 10^{-3}$.

The set of complex exponentials can not only describe the HBT microwave behavior, but can also give approximate information on the initial values of the extrinsic elements for the iterative determination of the equivalent circuit. The measurement frequency range is from 0.2 to 18 GHz. The frequency step (Δf) is taken as 0.2 GHz. The total sampled data number is 90, and the angular frequency is related to the sampling point by

$$\omega_k = 2\pi \cdot \Delta f \cdot k \quad (8)$$

where k denotes the k th sampling point, and ω_k is the k th sampling point in the angular frequency.

Following the GPOF method [10]–[12], we obtain various residues and poles to express the S -parameters as the sum of complex exponentials. Fig. 2 show the comparison between the measured and calculated S -parameters. The solid lines indicate the measured values and crosses indicate the calculated values by the sum of complex exponentials using the GPOF method.

The total S -parameters are then converted to the Z -parameters. From (1)–(4), we obtain

$$\begin{aligned} \text{Re}(Z_{11k}^{\text{total}} - Z_{12k}^{\text{total}}) \\ = g_1(\omega_k) = \frac{(C_{\text{ex}} + C_{bc})R_bC_{bc}}{(C_{\text{ex}} + C_{bc})^2 + \omega_k^2(R_bC_{bc}C_{\text{ex}})^2} + R_B \end{aligned} \quad (9a)$$

$$\begin{aligned} \text{Im}(Z_{11k}^{\text{total}} - Z_{12k}^{\text{total}}) \\ = g_2(\omega_k) = \frac{-\omega_kR_b^2C_{bc}^2C_{\text{ex}}}{(C_{\text{ex}} + C_{bc})^2 + \omega_k^2(R_bC_{bc}C_{\text{ex}})^2} + \omega_kL_B \end{aligned} \quad (9b)$$

$$\begin{aligned} \text{Re}(Z_{22k}^{\text{total}} - Z_{21k}^{\text{total}}) \\ = g_3(\omega_k) = \frac{-R_bC_{bc}C_{\text{ex}}}{(C_{\text{ex}} + C_{bc})^2 + \omega_k^2(R_bC_{bc}C_{\text{ex}})^2} + R_C, \end{aligned} \quad (9c)$$

By approximating $\text{Re}(Z_{11k}^{\text{total}} - Z_{12k}^{\text{total}})$, $\text{Im}(Z_{11k}^{\text{total}} - Z_{12k}^{\text{total}})$, and $\text{Re}(Z_{22k}^{\text{total}} - Z_{21k}^{\text{total}})$ individually as the sum of complex exponentials, namely, $f_1(k)$, $f_2(k)$ and $f_3(k)$, we have

$$\text{Re}(Z_{11k}^{\text{total}} - Z_{12k}^{\text{total}}) = f_1(k) = \sum_{i=1}^{M_1} R_i z_i^k \quad (10a)$$

$$\text{Im}(Z_{11k}^{\text{total}} - Z_{12k}^{\text{total}}) = f_2(k) = \sum_{i=1}^{M_2} R_i z_i^k \quad (10b)$$

$$\text{Re}(Z_{22k}^{\text{total}} - Z_{21k}^{\text{total}}) = f_3(k) = \sum_{i=1}^{M_3} R_i z_i^k \quad (10c)$$

where $M_1 = 11$, $M_2 = 10$, and $M_3 = 9$. The values of R_i and z_i for $f_1(k)$, $f_2(k)$ and $f_3(k)$ are given in Table I, respectively.

Equating (9a)–(9c) with (10a)–(10c), and assuming up to the second derivative continuity, the following simultaneous equations are obtained:

$$g_i(\omega_k)|_{k=0} = f_i(k)|_{k=0}, \quad i = 1, 2, 3 \quad (11a)$$

$$\frac{\partial^2 g_1(\omega_k)}{\partial^2 k} \Big|_{k=0} = \frac{\partial^2 f_1(k)}{\partial^2 k} \Big|_{k=0} \quad (11b)$$

$$\frac{\partial^3 g_2(\omega_k)}{\partial^3 k} \Big|_{k=0} = \frac{\partial^3 f_2(k)}{\partial^3 k} \Big|_{k=0} \quad (11c)$$

$$\frac{\partial^2 g_3(\omega_k)}{\partial^2 k} \Big|_{k=0} = \frac{\partial^2 f_3(k)}{\partial^2 k} \Big|_{k=0}. \quad (11d)$$

In order to obtain a high-order derivatives of $f_1(k)$, $f_2(k)$ and $f_3(k)$, we apply the central-difference approximation

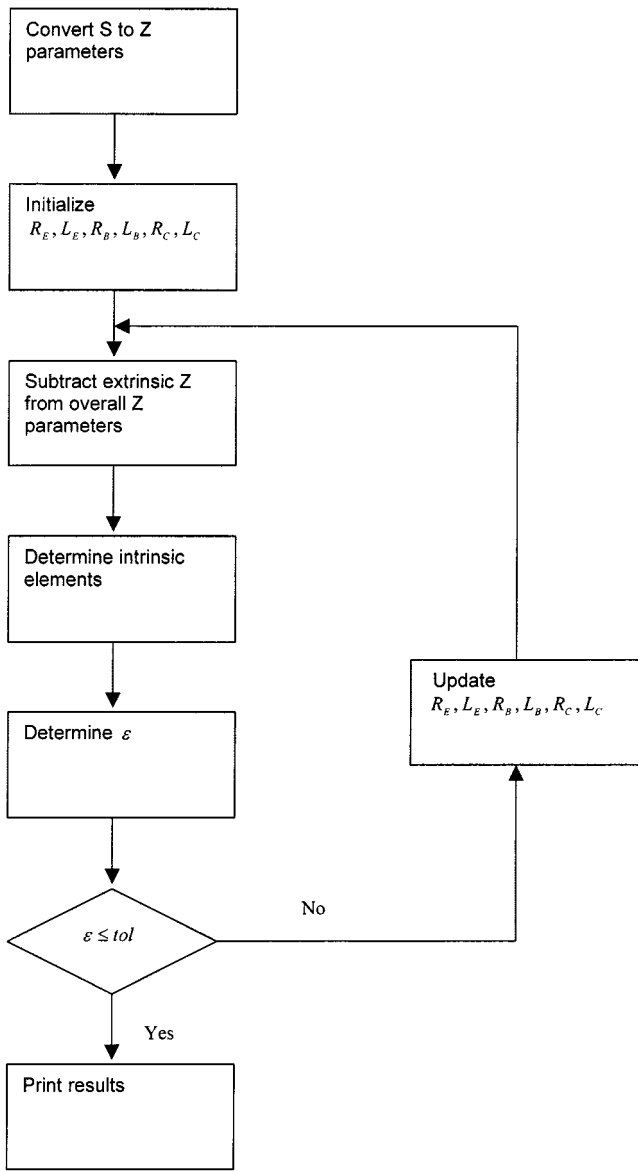


Fig. 3. Algorithm.

method [13] with an error of order h^4 . Thus, the truncation error for the first-order central-difference approximation is $1/30h^4f_i^{(5)}$. Similarly, the truncation error for the second-order central-difference approximation is $1/90h^4f_i^{(6)}$, and the truncation error for the third-order central-difference approximation is $7/120h^4f_i^{(7)}$, where h is the step size, and $f_i^{(n)}$ ($n = 5, 6, 7$) denotes the n th-order derivative of the function f_i ($i = 1, 2, 3$).

Based on (11a)–(11d) and by using the appropriate Taylor series expansions and the numerical differentiation approximation to obtain the high-order derivatives of $f_1(k)$, $f_2(k)$ and $f_3(k)$, the values of R_B , L_B , and R_C can be obtained. The values of R_B , L_B , and R_C are found to be $R_B = 8.012 \Omega$, $L_B = 44.895$ pH, and $R_C = 8.990 \Omega$.

V. RESULTS AND DISCUSSIONS

In our method, the iterative algorithm is the same as that in [8]. The initial values of R_B , L_B , and R_C are determined as in the above section. The initial values of the three remaining

TABLE II
EXTRACTED VALUES OF EXTRINSIC AND INTRINSIC ELEMENTS

$R_E(\Omega)$	$L_E(pH)$	$R_B(\Omega)$	$L_B(pH)$	$R_C(\Omega)$	$L_C(pH)$	
5.346	15.180	8.753	45.534	9.576	50.410	
$R_{be}(\Omega)$	$C_{be}(pF)$	$C_{ex}(pF)$	$C_{bc}(pF)$	$R_b(\Omega)$	α_0	$\tau(ps)$
4.203	0.649	0.023	0.047	8.673	0.951	4.809

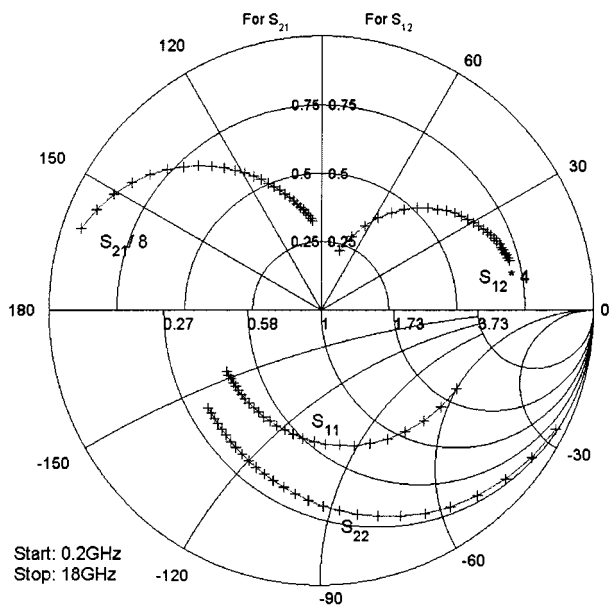


Fig. 4. Comparison of S -parameters between measured and simulated data. Crosses indicate measured values and solid lines indicate simulated values.

extrinsic elements R_E , L_E , and L_C are arbitrarily selected as $R_E = 1.0 \Omega$, $L_E = 10$ pH, and $L_C = 20$ pH. All element values are updated by Levenberg–Marquardt method [8], [14] in the iterations. The flowchart is given in Fig. 3.

Our modeled AlGaAs/GaAs HBT contains two emitter fingers, each of which is 2-mm wide and 10-mm long. The biasing condition is $I_C = 15$ mA and $V_{CE} = 3$ V, and the frequency range is from 0.2 to 18 GHz. In the numerical differentiation approximation, we select the step size (h) as 0.01. The element values extracted using our technique are shown in Table II. The comparison between the measured and simulated S -parameters under the proposed technique for the AlGaAs/GaAs HBT is presented in Fig. 4. A close agreement between the measured and simulated S -parameters is noted from these figures.

In the conventional methods, the selection of the initial values sometimes affects the final results. In our new method, the reliable initial values of some extrinsic elements are determined automatically from the set of complex exponentials. Therefore, the optimization efficiency and accuracy are greatly improved. As compared with a pure optimization process, our optimization process based on the GPOF method can result in less data

TABLE III
COMPARISON OF THE RMS ERRORS BETWEEN SIMULATED AND MEASURED DATA WITH THE DIFFERENT VALUES OF M

	RMS Err. (%)
$M_1=8, M_2=10, M_3=9$	2.02
$M_1=13, M_2=10, M_3=9$	1.48
$M_1=11, M_2=8, M_3=9$	1.56
$M_1=11, M_2=12, M_3=9$	2.03
$M_1=11, M_2=10, M_3=7$	1.98
$M_1=11, M_2=10, M_3=11$	1.91
$M_1=11, M_2=10, M_3=9$	0.81

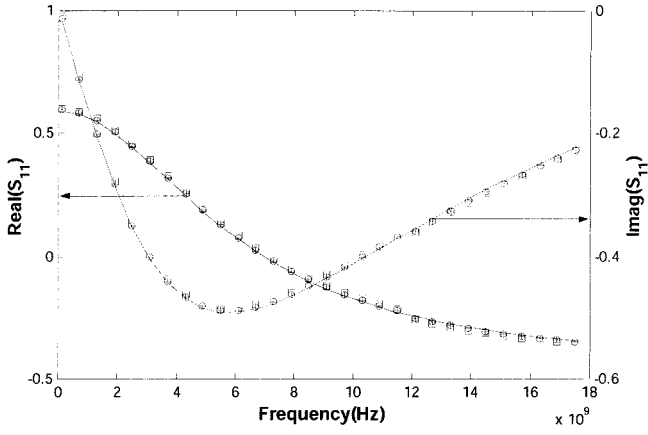


Fig. 5. Comparison of S_{11} between measured and simulated data. Solid lines indicate measured values and others indicate calculated values using our new technique (crosses: $h = 0.01$, circles: $h = 0.001$, squares: $h = 0.0001$).

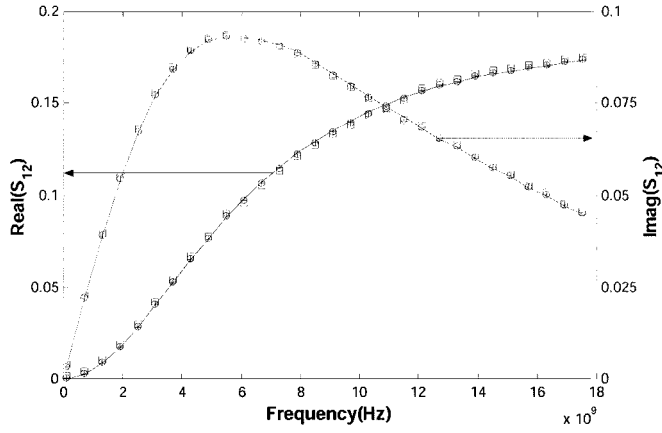


Fig. 6. Comparison of S_{12} between measured and simulated data. Solid lines indicate measured values and others indicate calculated values using our new technique (crosses: $h = 0.01$, circles: $h = 0.001$, squares: $h = 0.0001$).

manipulation and storage. Moreover, it can also lead to faster computation.

It is observed that M and h have some effects on the final equivalent-circuit parameters and simulation results. If unsuitable M values are used, the simulation results will be poor. Table III shows the rms errors between measured and simulated data with the different values of M . Figs. 5–8 show the comparison of the S -parameters between the measured and simulated data with the different step size (h). From these figures, it is noted that the selection of the step size has a great effect on the

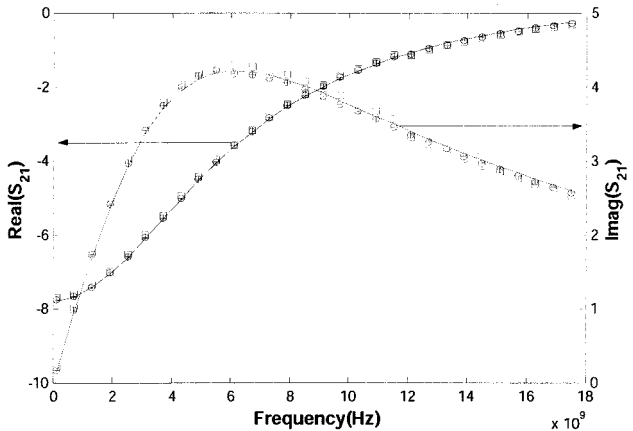


Fig. 7. Comparison of S_{21} between measured and simulated data. Solid lines indicate measured values and others indicate calculated values using our new technique (crosses: $h = 0.01$, circles: $h = 0.001$, squares: $h = 0.0001$).

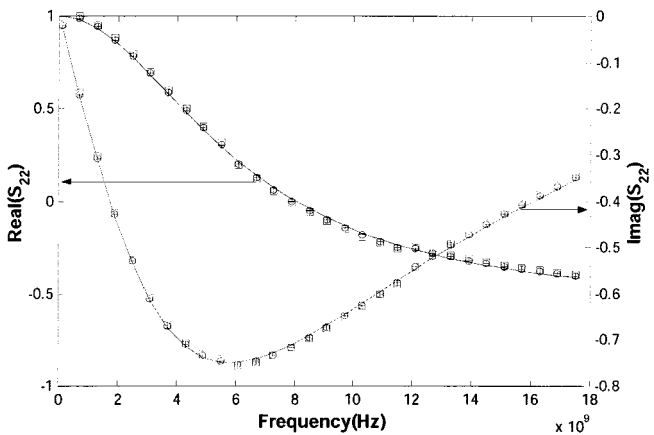


Fig. 8. Comparison of S_{22} between measured and simulated data. Solid lines indicate measured values and others indicate calculated values using our new technique (crosses: $h = 0.01$, circles: $h = 0.001$, squares: $h = 0.0001$).

final simulation results. For $h = 0.01$ and $h = 0.001$, the extracted model element values are the same and excellent agreement between simulated and measured data can be obtained. However, for $h = 0.0001$, the extracted model element values are different and the final simulation results are also different.

VI. CONCLUSION

A novel approach for the HBT small-signal equivalent-circuit parameters extraction has been introduced in this paper. The relation between extrinsic and intrinsic elements is analyzed in depth and the detailed expressions are obtained. A new technique for describing the high-frequency behavior of microwave devices by using a set of complex exponentials based on GPOF method is proposed. Excellent agreements between the measured and simulated values are achieved.

REFERENCES

- [1] R. J. Trew, U. K. Mishra, W. L. Pribble, and J. F. Jensen, "A parameter extraction technique for heterojunction bipolar transistors," in *IEEE MTT-S Int. Microwave Symp. Dig.*, June 1989, pp. 897–899.
- [2] D. Costa, W. U. Liu, and J. S. Harris, "Direct extraction of the AlGaAs/GaAs heterojunction bipolar transistor small signal equivalent circuit," *IEEE Trans. Electron Devices*, vol. 38, pp. 2018–2023, Sept. 1991.

- [3] D. R. Pehlke and D. Pavlidis, "Evaluation of the factors determining HBT high frequency performance by direct analysis of S -parameter data," *IEEE Trans. Microwave Theory Tech.*, vol. 40, pp. 2367–2373, Dec. 1992.
- [4] S. A. Maas and D. Tait, "Parameter-extraction method for heterojunction bipolar transistors," *IEEE Microwave Guided Wave Lett.*, vol. 2, pp. 502–504, Dec. 1992.
- [5] C.-J. Wei and J. C. M. Hwang, "Direct extraction of equivalent circuit parameters for heterojunction bipolar transistors," *IEEE Trans. Microwave Theory Tech.*, vol. 43, pp. 2035–2040, Sept. 1995.
- [6] S. J. Spiegel, D. Ritter, R. A. Hamm, A. Feygenson, and P. K. Smith, "Extraction of the InP/GaInAs heterojunction bipolar transistor small-signal equivalent circuit," *IEEE Trans. Electron Devices*, vol. 42, pp. 1059–1064, June 1995.
- [7] U. Schaper and B. Holzapfi, "Analytical parameter extraction of the HBT equivalent circuit with T-like topology from measured S -parameters," *IEEE Trans. Microwave Theory Tech.*, vol. 43, pp. 493–498, Mar. 1995.
- [8] B.-L. Ooi, M.-S. Leong, and P.-S. Kooi, "A novel approach for determining the GaAs MESFET small-signal equivalent-circuit elements," *IEEE Trans. Microwave Theory Tech.*, vol. 45, pp. 2084–2088, Dec. 1997.
- [9] K. Shirakawa, H. Oikawa, T. Shimura, Y. Kawasaki, Y. Ohashi, T. Saito, and Y. Daido, "An approach to determining an equivalent circuit for HEMT's," *IEEE Trans. Microwave Theory Tech.*, vol. 43, pp. 499–503, Mar. 1995.
- [10] Y. Hua and T. K. Sarkar, "Generalized pencil-of-function method for extracting the poles of an electromagnetic system from its transient response," *IEEE Trans. Antennas Propagat.*, vol. 37, pp. 229–234, Feb. 1989.
- [11] G. H. Golub and C. F. Van Loan, *Matrix Computations*. Baltimore, MD: The Johns Hopkins Univ. Press, 1983.
- [12] M. L. James, G. M. Smith, and J. C. Wolford, *Applied Numerical Methods for Digital Computation*. New York: Harper Collins, 1993.
- [13] K. Levenberg, "A method for the solution of certain problems in least squares," *Q. Appl. Math.*, vol. 2, pp. 164–168, 1944.
- [14] D. Marquardt, "An algorithm for least squares estimation of nonlinear parameters," *SIAM J. Appl. Math.*, vol. 11, pp. 431–441, 1963.

B. L. Ooi, photograph and biography not available at time of publication.

T. S. Zhou, photograph and biography not available at time of publication.

P. S. Kooi, photograph and biography not available at time of publication.